ANNUAL PERFORMANCE PREDICTION OF A HYBRID BRAYTON THERMOSOLAR PLANT

Merchán R.P.*, Santos M.J., Medina A., and Calvo Hernández A.
Department of Applied Physics,
University of Salamanca,
Salamanca, 37008, Spain,
*E-mail: rpmerchan@usal.es

ABSTRACT

We present a thermodynamic model for the prediction of the performance records of a solar hybrid gas turbine power plant, with the aim to deliver to the grid an steady power output. The overall thermal efficiency depends on the efficiencies of the involved subsystems and the required heat exchangers in a straightforward analytical way. Numerical values for input parameters are taken from a central tower heliostat field recently developed near Seville, Spain. Real curves for irradiance and external temperature are taken. The values of several variables in yearly terms are predicted and the fuel consumption assuming natural gas is estimated, as well as greenhouse emissions. Moreover, we present an analysis of the losses coming from each plant subsystem. This kind of analysis can contribute to improve the design of these facilities in order to get better performance.

INTRODUCTION

During the last years several experimental projects have tried to develop hybrid solar gas turbine technologies in which concentrated solar power coming from a central receiver plant is used to heat pressurized air that performs a Brayton cycle [1]. This technology is suitable for regions with favorable solar irradiance conditions, usually linked to water shortage. These power plants can be combined with other cycles in order to improve their overall efficiency. The term hybrid refers to the fact that during low solar radiation periods a combustion chamber ensures an stable power release to the electricity grid and avoids the use of storage systems. Apart from R+D projects, prototypes, and experimental installations, several research works have been published in the last times. Some of them make use of commercial simulation environments or in-house developed software which allows a detailed description of all plant components and specific calculations on the solar subsystem [2]. But, in this way, it is not easy to extract direct physical information about the main losses sources in the plant and to plan global strategies for the optimization of the plant design and operation as a whole. This is why we follow next modus operandi instead of previous one.

On the other hand, there are several theoretical works starting from the Brayton ideal cycle that thereafter include refinements in order to recover realistic output records [3; 4; 5]. Usually, in these works the model for the concentrated solar subsystem, although including the main heat transfer losses, is simple. This favors to obtain closed analytical expressions for thermal efficiencies and power output in terms of a reduced number of parameters, with clear physical meaning each, and then check the model predictions for particular design point conditions, with fixed values of solar irradiance and ambient temperature. Also it allows to guide optimization strategies and to suggest where an investment in enhancing the losses gives more results. Thereby, this paper helps to improve the design of these facilities, getting information about the main irreversibility sources and the bottlenecks of the overall plant efficiency.

THERMODYNAMIC PLANT MODEL

We consider a central tower hybrid solar installation as depicted in Fig.1. A single step recuperative closed Brayton cycle is hybridized in order to release to the grid an stable power output, independent of solar irradiance conditions. The model is simple and uses a reduced number of parameters with a clear physcial meaning each. Thus, analytical expressions can be reached.

Our hybrid plant consists of three main susbsystems: a solar collector, a combustion chamber, and a heat engine. The whole system receives two energy inputs. On the one hand, a heat input, GA_a, comes from the sun, where G is the direct solar irradiance and A_a, the aperture area of the solar field. The direct solar irradiance is not constant over time, but it depends on the sun position during the day, the meteorological conditions and the seasonal fluctuations. The solar useful heat flux, $|\dot{Q}'_{HS}|$, is transferred to the working fluid through a solar receiver, considered as non-ideal heat exchanger with effectiveness ε_{HS}. So the effective solar heat flux received in the heat engine is $|\dot{Q}_{HS}| = \varepsilon_{HS}|\dot{Q}'_{HS}|$. The efficiency of the solar collector, η_s, is then defined as the ratio between the heat useful flux it provides, $|\dot{Q}'_{HS}|$, and solar energy input: $\eta_S = \frac{|\dot{Q}'_{HS}|}{GA_a} = \frac{|\dot{Q}_{HS}|}{\varepsilon_{HS} GA_a}$.

On the other hand, the energy input at the combustion chamber is $\dot{m}_f Q_{LHV}$, being $\dot{m}_f$ the fuel mass flow rate and Q_{LHV}, its corresponding lower heating value. The fuel mass rate will be also considered as time dependent because it should compensate solar irradiance fluctuations. Combustion chamber releases a heat rate $|\dot{Q}'_{HC}|$ to its heat exchanger, whose effectiveness is

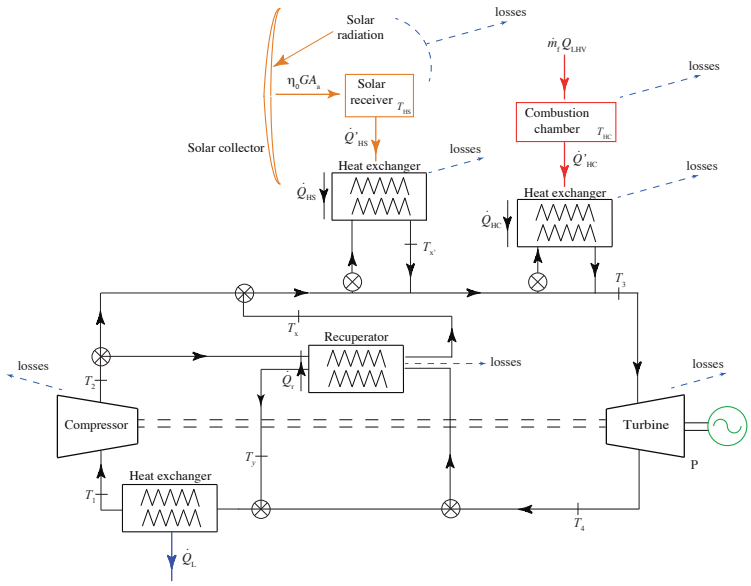

Figure 1: Scheme of the hybrid solar gas-turbine plant considered.

$\varepsilon_{HC} = |\dot{Q}_{HC}|/|\dot{Q}'_{HC}|$, because the fuel is not injected in the air itself since an externally fired gas turbine (EFGT) is being assumed. Finally, the working fluid in the heat engine receives a heat flux, $|\dot{Q}_{HC}|$, from combustion chamber. Therefore, combustion chamber efficiency is given by: $\eta_C = \frac{|\dot{Q}'_{HC}|}{\dot{m}_f Q_{LHV}} = \frac{|\dot{Q}_{HC}|}{\varepsilon_{HC}\dot{m}_f Q_{LHV}}$.

The heat engine delivers a mechanical power output, P, independent of solar radiation fluctuations, and releases a heat flux to the ambient $|\dot{Q}_L|$. The ratio between net power output and heat flux tranferred to the working fluid defines heat engine efficiency: $\eta_H = \frac{P}{|\dot{Q}_{HS}|+|\dot{Q}_{HC}|}$. There is an internal heat transfer in a possible recuperator, denoted as $|\dot{Q}_r|$.

Global thermal efficiency of the plant.

The overall thermal efficiency, η, is defined as the quotient between the net mechanical power output and the total heat input rate needed to produce it: $\eta = \frac{P}{GA_a + \dot{m}_f Q_{LHV}}$. Using the ratio of the solar heat rate that the working fluid absorbs with respect to the total heat input, called solar share fraction, $f = |\dot{Q}_{HS}|/(|\dot{Q}_{HS}| + |\dot{Q}_{HC}|)$, and the definitions above, it can be expressed as:

$$\eta = \eta_S \eta_C \eta_H \left[\frac{\varepsilon_{HS}\varepsilon_{HC}}{\eta_C \varepsilon_{HC} f + \eta_S \varepsilon_{HS}(1-f)} \right] \qquad (1)$$

There is another interesting performance, denominated fuel conversion rate, that relates power output to required heat with an economical cost associated (fuel burned): $r_e = P/(\dot{m}_f Q_{LHV})$. It does not represent a thermodynamic efficiency because it is defined in the range [0,∞]:

$$r_e = \frac{\eta \eta_S \eta_H \varepsilon_{HS}}{\eta_S \eta_H \varepsilon_{HS} - \eta f} \qquad (2)$$

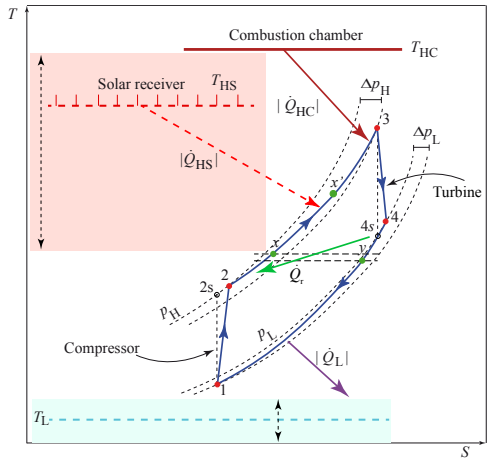

Figure 2: T-S diagram of the irreversible Brayton cycle experienced by the working fluid.

Modeling the solar and combustion subsytems

A simple model for the concentrating solar system is considered and based on the concept of optical efficiency, η_0, which indicates how good is reflexion towards solar concentrator. The solar efficiency can be derived as the difference between η_0 and two terms linked, one to conduction and convection losses: linear in temperature differences with a coefficient $h_2 = U_L/(\eta_0 GC)$, and the other one to radiation losses: fourth power of temperature with a coefficient $h_1 = \alpha\sigma/(\eta_0 GC)$. C represents the concentration ratio $C = A_a/A_r$, A_r the absorber area, σ the Stefan-Boltzmann constant, α the effective emissivity of the collector, and U_L the convective heat loss coefficient.

$$\eta_S = \frac{|\dot{Q}'_{HS}|}{GA_a} = \eta_0[1 - h_1 T_L^4(\tau_{HS}^4 - 1) - h_2 T_L(\tau_{HS} - 1)] \qquad (3)$$

τ_{HS} refers to $\tau_{HS} = T_{HS}/T_L$, the quotient between the solar collector working temperature, T_{HS}, and the ambient temperature, T_L.

If a particular fuel is chosen, the efficiency of the combustion chamber, η_C, can be taken as a constant parameter, without considering fluctuations due to the composition of the fuel, its temperature, the fuel-air equivalence ratio and others. With the objective of cancelling the fluctuations in G, burned fuel mass should change with time: $\dot{m}_f = \frac{\dot{m} c_w (T_3 - T_{x'})}{\eta_C Q_{LHV} \varepsilon_{HC}}$, where $\dot{m}$ represents the working fluid mass flow, c_w its specific heat, T_3 the turbine inlet temperature, and $T_{x'}$ the working fluid temperature after solar heat input.

Modeling the Brayton gas-turbine subsystem

A mass rate of an ideal gas undergoes an irreversible closed recuperative Brayton cycle, whose T-S diagram is shown in Fig.2. It can be seen that both the working temperature of the solar receiver and that of the ambient are fluctuating quantities. Though it is a debatable hypothesis, a constant averaged specific heat, c_w, is supposed because it allows to find the influence of parameters and losses clearly and to obtain systematic expressions. The process steps are:

1. The working gas is first compressed $(1 \rightarrow 2)$ in a non-ideal compressor, whose isentropic efficiency is ε_c, from a temperature T_1 up to T_2.
2. Then, the gas is heated by three means $(2 \rightarrow 3)$. First of all, a recuperator releases heat, raising its temperature from T_2 to T_x. Next, solar collector increases the temperature up to $T_{x'}$ and, finally, combustion chamber completes heat input. Thus, gas temperature after heating process, T_3, is approximately constant (it varies only with ambient temperature fluctuations). The recuperator presents an effectiveness given by ε_r. A new parameter, ρ_H, is employed to measure the pressure decrease in the process $2 \rightarrow 3$.
3. At the turbine $(3 \rightarrow 4)$, whose isentropic efficiency is ε_t, the gas is expanded and cooled irreversibly from its maximum temperature T_3 to T_4 .
4. Finally the working fluid recovers its initial conditions $(4 \rightarrow 1)$, releasing heat by two ways: first, with the recuperator (T_y) and, afterwards, using a heat exhanger which transfers heat to the surroundings, with effectiveness ε_L. By analogy with the process $2 \rightarrow 3$, a pressure drop, ρ_L, can be defined.

In this way, the heat input rates are given by the following equations, as a function of all the temperatures above:

$$|\dot{Q}_H| = |\dot{Q}_{HS}| + |\dot{Q}_{HC}| = \dot{m} c_w (T_3 - T_x) \tag{4}$$

$$|\dot{Q}_{HS}| = \dot{m} c_w \left(T_{x'} - T_x\right) = f|\dot{Q}_H| \tag{5}$$

$$|\dot{Q}_{HC}| = \dot{m} c_w \left(T_3 - T_{x'}\right) = (1-f)|\dot{Q}_H| \tag{6}$$

$$|\dot{Q}_L| = \dot{m} c_w (T_y - T_1) \tag{7}$$

These temperatures can be expressed in terms of the main parameters and irreversibilities of the plant, as it is deduced in previous works ([3; 4]) by our group. Therefore, the power output, $P = |\dot{Q}_H| - |\dot{Q}_L|$, the thermal efficiency of the Brayton heat engine, $\eta_H = P/|\dot{Q}_H|$, and the overall plant efficiency, Eq.(1), have analytical expressions that can be evaluated for any particular parameters arrangement.

NUMERICAL IMPLEMENTATION

Numerical implementation: parameters

In a previous work [3] this model was validated in fixed solar irradiance and fixed ambient temperature conditions. We chose a thermosolar hybrid Brayton plant, located in Sanlúcar La Mayor, near Seville (Spain) which is part of SOLUGAS project (Abengoa) [1], but the model can be applied to any plant of such characteristics. In this project, a turbine with a power output of $4.6\,MW$ is employed: *Mercury 50*, Caterpillar [6]. The working fluid is supposed pressurized air, but others can be employed; for instance, CO_2, helium and other noble gases [7]. All the involved parameters take the values stated in [3; 4]. The agreement between data from manufacturer and results from the model is good, as set forth in [3; 4].

Once comparison with turbine data is completed, it should be done the same for solar data. But results from SOLUGAS Project are not completely published yet, so several standard values of combustion chamber and solar parameters are supposed [1; 8]. Natural gas has been assumed as fuel, whose lower heating value is $Q_{LHV} = 47.141\,MJ/kg$, and the design point conditions were taken from Abengoa [1] at $G = 860\,W/m^2$ and $T_L = 288\,K$. This information is collected in Table 1. Turbine inlet temperature, T_3, and power output, P, have values within the expected ranges. Moreover, the estimated efficiencies are in right accordance with published values for this kind of plants [8].

Solar plant parameters at design point		
$\eta_0 = 0.73$	$\varepsilon_{HS} = 0.78$	$G = 860\,W/m^2$
$\alpha = 0.1$	$C = 425.2$	$U_L = 5\,W/(m^2K)$
Combustion related parameters		
$\eta_C = 0.98$	$T_{HC} = 1430\,K$	$\varepsilon_{HC} = 0.98$
Thermal cycle temperatures (K)		
$T_1 = 294$	$T_2 = 590$	$T_x = 822$
$T_{x'} = 1027$	$T_3 = 1422$	$T_4 = 890$
$T_y = 657$		
Estimated output parameters		
$f = 0.341$	$\dot{m}_f = 0.172\,kg/s$	$P = 4.647\,MW$
Estimated efficiencies		
$\eta_H = 0.393$	$\eta_S = 0.698$	$\eta = 0.300$

Table 1: Simulation predictions of our model for the main parameters of the thermosolar plant developed for SOLUGAS Project.

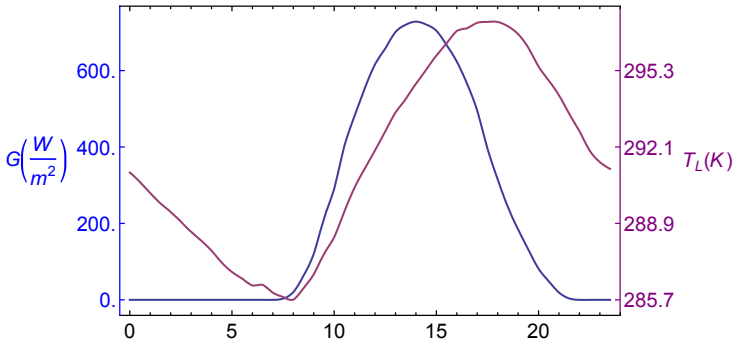

Figure 3: Annual mean solar direct irradiance (blue) and annual mean ambient temperature (purple) in UTC time.

Numerical implementation: annual performance

With the goal of simulating the performance of the plant in annual terms, a data source of solar direct irradiance (G) and ambient temperature (T_L) is required. We took metereological data from Meteosevilla [9] database, taking G and T_L each half an hour in Sanlúcar La Mayor.

The main objective of this work is to perform an annual study of the behaviour of the main variables (a seasonal study was recently developed in [4; 5] by our group). For that, a year is divided into four seasons: winter, spring, summer, and au-

Subsystem		(A) Real (Operating point)	(B) Ideal heat exchangers	(C) Ideal solar part	(D) Ideal Brayton cycle	(E) Ideal complete system
Solar part	YS	$\eta_0 = 0,65$ $\alpha = 0.1$ $U_L = 5$ $\varepsilon_{HS} = 0.78$	$\varepsilon_{HS} = 1$	$\eta_0 = 1$ $\alpha = 0$ $U_L = 0$ $\varepsilon_{HS} = 1$		$\eta_0 = 1$ $\alpha = 0$ $U_L = 0$ $\varepsilon_{HS} = 1$
	NS	$\varepsilon_{HS} = 0$				
Combustion part		$\eta_C = 0.98$ $\varepsilon_{HC} = 0.98$	$\varepsilon_{HC} = 1$		$\varepsilon_{HC} = 1$	$\eta_C = 1$ $\varepsilon_{HC} = 1$
Brayton part		$\varepsilon_t = 0.885$ $\varepsilon_c = 0.815$ $\varepsilon_L = 0.985$ $\rho_H = 0.975$ $\rho_L = 0.97$	$\varepsilon_L = 1$		$\varepsilon_t = 1$ $\varepsilon_c = 1$ $\varepsilon_L = 1$ $\rho_H = 1$ $\rho_L = 1$	$\varepsilon_t = 1$ $\varepsilon_c = 1$ $\varepsilon_L = 1$ $\rho_H = 1$ $\rho_L = 1$
	YR	$\varepsilon_r = 0.775$			$\varepsilon_r = 1$	$\varepsilon_r = 1$
	NR	$\varepsilon_r = 0$				

Table 2: Values of plant parameters in the five models.

tumn; each of them is modeled by three representative days, corresponding to the 3 months that form a season. Selected days present a certain meteorological and solar stability. Solar direct irradiance and ambient temperature are averaged in every season. Those averages contribute to smooth noise in solar direct irradiance (G) and in ambient temperature (T_L).

With the help of our own software, developed in programming language Mathematica®, calculations are made seasonally in order to obtain the time evolution in a day of the whole set of plant variables. These results can be integrated over time in 24 hours. Once computation is done in every season, annual means are calculated for all the outputs of the plant, such as η, f or P, involving the four seasons. It should be noted that this procedure leads to an annually averaged day.

In Figure 3 it can be seen the smooth curve of the evolution of annual G and T_L during a day. Solar irradiance is zero overnight and has a parabolic shape during the day. Meanwhile, ambient temperature is minimal at dawn and rises linearly until afternoon, when it begins to decrease.

It is significant that some variables are averaged for sunshine hours: η_S, f, T_{HS}, and G (initial data). While, the rest are averaged during the whole day: η, r_e, η_H, P, T_y, and T_L (initial data). The mean surroundings temperature value is $T_L = 291.575\,K$, while mean annual solar irradiance is $G = 457.874\,W/m^2$, a realistic value (about half of the design point for the SOLUGAS project).

RESULTS

In this section an annual study is performed at operating point, varying solar irradiance and ambient temperature. Four situations are analyzed according to the existence or not existence of solar input and recuperator. From the case in which both "with" are kept: with solar input and with recuperation (YSYR) to the case: without solar input and without recuperation (NSNR). Intermediate states are: without solar input and with recuperation (NSYR) and with solar input and without recuperation (YSNR). We shall take as base case YSYR. The other cases will be specifically mentioned. Starting from operating point, other four configurations can be investigated with the goal of examining possible plant improvements over the real operating point of the plant (see Table 2): ideal heat exchangers, ideal solar part, ideal Brayton cycle, and ideal complete system (ordered from worst to best performance).

Operating point	With recuperation			Without recuperation		
	Solar input	No solar input	Relative differences	Solar input	No solar input	Relative differences
η	0.342	0.367	−6.937 %	0.250	0.263	−4.747 %
r_e	0.406	0.367	9.540 %	0.283	0.263	7.392 %
η_S	0.586	–	–	0.620	–	–
η_H	0.383	0.383	0.077 %	0.274	0.274	0.043 %
f	0.164	0	–	0.123	0	–
$T_{HS}(K)$	946.598	–	–	730.124	–	–
$T_y(K)$	663.469	663.329	0.021 %	888.64	888.028	0.069 %
$P(MW)$	4.476	4.469	0.161 %	4.377	4.370	0.162 %

Table 3: Performance records annual means: operating point.

Since our model is analytical and simple, it enables to identify the irreversibilities or losses in any subsystem, which constitutes an important advantage.

Operating point

When results are obtained, some parameters change their values with respect to numerical implementation. This happens because variables are too optimistic at design point. As we want to do a study as close as possible to reality, we choose realistic values for the whole set of parameters. Talking about solar part, the optical efficiency is now $\eta_0 = 0.65$, considered as an annually averaged reasonable value. When there is no solar input, the solar heat exchanger effectiveness is set to zero. In this point it should be noted that there are always two values for the recuperator effectiveness. This corresponds to the cases with and without recuperator. When $\varepsilon_r = 0.775$ or $\varepsilon_r = 1$, we work with recuperator and if $\varepsilon_r = 0$, the recuperator is not employed.

Results for most important performance records are included in Table 3. In addition, the relative differences between variables with solar input and without it are calculated, referring to the case of not solar input. At operating point, keeping combustion chamber temperature fixed ($T_{HC} = 1430\,K$), a power output of $4.47\,MW$, very close to that at design point ($P_{dp} = 4.6\,MW$), can be achieved. Solar collector temperature can reach a value of $T_{HS} = 946.6\,K$.

Exhaust temperature presents a high value both in the case of solar input and recuperation and in the case of solar input and no recuperation: $T_{y,YRYS} = 663.5\,K$ and $T_{y,NRYS} = 888.6\,K$, respectively. This is important to take advantage of residual heat cycle with cogeneration or bottoming cycles. As these temperatures are high, a bottoming Rankine cycle can be used and, thereby,

Ideal heat exchangers	With recuperation			Without recuperation		
	Solar input	No solar input	Relative differences	Solar input	No solar input	Relative differences
η	0.365	0.386	−5.558 %	0.265	0.275	−3.795 %
r_e	0.441	0.386	14.383 %	0.301	0.275	9.521 %
η_S	0.585	–	–	0.622	–	–
η_H	0.394	0.394	0 %	0.281	0.281	0 %
f	0.208	0	–	0.152	0	–
$T_{HS}(K)$	948.998	–	–	712.234	–	–
$T_y(K)$	656.354	656.354	0 %	898.406	898.406	0 %
$P(MW)$	4.668	4.668	0 %	4.668	4.668	0 %

Table 4: Performance records annual means: ideal heat exchangers.

Ideal solar part	With recuperation			Without recuperation		
	Solar input	No solar input	Relative differences	Solar input	No solar input	Relative differences
η	0.370	0.367	0.808 %	0.265	0.263	0.567 %
r_e	0.479	0.367	30.491 %	0.311	0.263	18.143 %
η_S	1	–	–	1	–	–
η_H	0.383	0.383	0.153 %	0.274	0.274	0.085 %
f	0.327	0	–	0.240	0	–
$T_{HS}(K)$	1014.25	–	–	794.991	–	–
$T_y(K)$	663.609	663.329	0.042 %	889.23	888.028	0.135 %
$P(MW)$	4.483	4.469	0.321 %	4.384	4.370	0.319 %

Table 5: Performance records annual means: ideal solar part.

power output and overall efficiency of the plant will increase and heat pollution will decrease.

Overall efficiency of the plant is larger if there is no solar input due to energy losses in solar part associated with high temperatures: $\eta = 0.367$, a 6.9% more. On the other hand, fuel conversion rate takes its larger value when there is solar input and recuperation: $r_e = 0.406$. It can be confirmed that the fuel conversion rate (r_e) is the overall thermal efficiency (η) in combustion mode. Solar collector efficiency is relatively good, $\eta_S = 0.586$; however, solar share is still small, $f = 0.164$.

Ideal heat exchangers

This case, shown in Table 4, is characterized by the ideality of the three heat exchangers (associated with solar receiver, combustion chamber and cold side): $\varepsilon_{HS} = 1$, $\varepsilon_{HC} = 1$ and $\varepsilon_L = 1$. The rest of variables continue taking the same values than at operating point. In this way, almost all variables enhance their values; for instance, overall eficiency increases until 0.365 and fuel conversion rate changes from 0.406 to 0.441. Exhaust temperature decreases with recuperator ($T_y = 656.354\,K$) and increases without it ($T_y = 898.406\,K$). It is important to stress that power output is the same in the four cases if ideal heat exchangers are considered ($P = 4.668\,K$). Solar collector temperature ($T_{HS} = 948.998\,K$) varies only slightly compared to the previous model.

Ideal Brayton cycle	With recuperation			Without recuperation		
	Solar input	No solar input	Relative differences	Solar input	No solar input	Relative differences
η	0.575	0.616	−6.676 %	0.421	0.442	−4.814 %
r_e	0.674	0.616	9.483 %	0.472	0.442	6.567 %
η_S	0.594	–	–	0.628	–	–
η_H	0.628	0.628	0 %	0.452	0.452	0 %
f	0.151	0	–	0.111	0	–
$T_{HS}(K)$	904.842	–	–	657.498	–	–
$T_y(K)$	531.597	531.597	0 %	784.338	784.338	0 %
$P(MW)$	7.988	7.988	0 %	7.988	7.988	0 %

Table 6: Performance records annual means: ideal Brayton cycle.

Ideal complete system	With recuperation			Without recuperation		
	Solar input	No solar input	Relative differences	Solar input	No solar input	Relative differences
η	0.628	0.628	0 %	0.452	0.452	0 %
r_e	0.792	0.628	25.988 %	0.522	0.452	15.677 %
η_S	1	–	–	1	–	–
η_H	0.628	0.628	0 %	0.452	0.452	0 %
f	0.301	0	–	0.218	0	–
$T_{HS}(K)$	971.015	–	–	722.12	–	–
$T_y(K)$	531.597	531.597	0 %	784.338	784.338	0 %
$P(MW)$	7.988	7.988	0 %	7.988	7.988	0 %

Table 7: Performance records annual means: ideal complete syst.

Ideal solar part

With this configuration (see Table 5) the optical efficiency value is $\eta_0 = 1$, both the effective emissivity and the convective heat loss coefficient are zero and solar collector heat exchanger is ideal: $\varepsilon_{HS} = 1$. Taking this into account, a solar collector efficiency of 1 is obtained directly from Eq.(3). The difference between solar input and no solar input is more than 30% in fuel conversion rate due to improvements on solar part. Precisely fuel conversion rate is larger than in the previous model, $r_e = 0.479$, and solar share increases its value considerably, $f = 0.367$, just as solar collector temperature: $T_{HS} = 1014.25\,K$. Since solar part is ideal, there is no losses associated with solar subsystem. So overall efficiency has to be greater with solar input than without it, which is fulfilled: $\Delta\eta = +0.808\%$. Exhaust temperatures ($T_{y,YRYS} = 663.6\,K$ and $T_{y,NRYS} = 889.2\,K$) are similar to the operating point and they do not change practically with and without solar input ($\Delta T_{y,YR} = 0.042\%$ and $\Delta T_{y,NR} = 0.135\%$).

Ideal Brayton cycle

Ideal Brayton cycle case means that all parameters from heat engine subsystem and also that of the combustion chamber heat exchanger are ideal. If we look at Table 6, we can see that overall efficiency ($\eta = 0.575$), fuel conversion rate ($r_e = 0.674$), heat engine efficiency ($\eta_H = 0.628$) and power output ($P = 7.988\,MW$) present so much higher values than in previous models. Such

improvements are very important, so here is the key for the optimization process. If we enhance enough the heat engine subsystem, we will achieve important and real upgrades in the general performance of the plant. Exhaust temperatures ($T_{y,YR} = 531.6\,K$ and $T_{y,NR} = 784.3\,K$) are identical with and without solar input and they are smaller thanks to the better performance and exploitation of the Brayton cycle. Power output takes the same values for the four cases, almost $8\,MW$.

Ideal complete system

At last, if we join the three last models and if we add ideality of the combustion chamber, the whole set of parameters take ideal values. Hence, results collected in Table 7 correspond to the best possible values of variables. It can be observed that while exhaust temperature ($T_{y,YR} = 531.6\,K$ and $T_{y,NR} = 784.3\,K$) remains constant with respect to ideal Brayton cycle, overall efficiency increases ($\eta = 0.628$). Fuel conversion rate rises up to $r_e = 0.792$, which is a very interesting value, and it is a 26% higher with solar input than without it. Moreover solar share reaches $f = 0.301$. Power output is also the same as in the ideal Brayton cycle model: $P = 7.988\,MW$ and solar collector efficiency is $\eta_s = 1$, like in the ideal solar part model. Now, heat engine efficiency is equal to overall efficiency, as can be deduced from Eq.(1).

Fuel consumption and emissions

Finally, it can be analyzed the specific natural gas consumption and the pollutant emissions associated with its burning, that are directly estimated thanks to the natural gas emission factors, collected in Table 8, where relative differences are calculated with respect to operating point. Specific emissions of carbon dioxide at normal performance (operating point, recuperation and solar input) are $CO_2 = 461.674\,kg/MWh$, whereas those of CH_4 and N_2O are $CH_4 = 8.735\,g/MWh$ and N_2O=$0.848\,g/MWh$, respectively. Also here it is observed that the leap ocurrs when ideal Brayton system is achieved, with almost a 40% of decrease in fuel consumption and pollutant emissions. Ideal heat exchangers and ideal solar part models give a smaller reduction of consumption: approximately 7% and 9%, respectively. Of course, the ideal complete system configuration presents the higher decrease, around 46%. Therefore the room for improvement is wide. If the complete system was ideal, specific carbon dioxide emission would be $CO_2 = 249.977\,kg/MWh$, which is a very promising result.

The data of estimated emissions should only be taken as a guide, because each plant could have particular technologies to reduce emissions or CO_2 capture mechanisms.

CONCLUSION

In this paper we have modeled a solar hybrid power plant based on a gas turbine following a closed Brayton cycle and incorporating the main losses sources: non-ideal turbine and compressor, pressure decays, heat exchangers, heat transfer losses in the solar collector, combustion inefficiencies, etc. The main contribution of this work is to get a simple and flexible thermodynamic model that offers a very good description of the plant, using a few variables, with clear physical meaning each. Thereby, we avoid to introduce a huge number of parameters and we allow to obtain analytical equations for all the thermal efficiencies and power output. Additionally, this study analyzes different plant configurations with the goal of highlighting where thermal energy losses are higher.

With recuperation and With solar input	Operating point	Ideal heat exchangers	Ideal solar part	Ideal Brayton cycle	Ideal complete system
$m_f\,(kg/MWh)$	186.569	173.516	169.781	112.204	101.019
$CO_2\,(kg/MWh)$	461.674	429.374	420.13	277.654	249.977
$CH_4\,(g/MWh)$	8.735	8.124	7.949	5.253	4.730
$N_2O\,(g/MWh)$	0.848	0.789	0.772	0.510	0.459
Relative differences	-	−6.996%	−8.998%	−39.859%	−45.854%

Table 8: Annual means of fuel specific consumption and of specific emissions in the five models, in the YSYR case.

Nowadays, these plants are not economically profitable, but if some improvements are achieved, probably they will be in the next future. This work tries to mark off and to reduce existing energy losses and, also, to reach improvements that lead to that sought profitability. Nevertheless, these plants are worth the effort from the ecological point of view, since they reduce pollutant emissions significantly, specifically greenhouse gases. As a result, hybrid thermosolar plants help mitigate anthropogenic intensification of climate change.

REFERENCES

[1] R. Korzynietz, M. Quero, and R. Uhlig. SOLUGAS-future solar hybrid technology. Technical report, SolarPaces, 2012.

[2] G. Barigozzi, G. Bonetti, G. Franchini, A. Perdichizzi, and S. Ravelli. Thermal performance prediction of a solar hybrid gas turbine. *Sol. Energy*, 86:2116–2127, 2012.

[3] D. Olivenza-León, A. Medina, and A. Calvo Hernández. Thermodynamic modeling of a hybrid solar gas-turbine power plant. *Energ. Convers. Manage.*, 93:435–447, 2015.

[4] M.J. Santos, R.P. Merchán, A. Medina, and A. Calvo Hernández. Seasonal thermodynamic prediction of the performance of a hybrid solar gas-turbine power plant. *Energ. Convers. Manage.*, 2016.

[5] M.J. Santos, R.P. Merchán, A. Medina, and A. Calvo Hernández. *Current Trends in Energy and Sustainability. 2015 Edition*, chapter Simulación Termodinámica de una planta termosolar híbrida tipo Brayton, pages 267–284. Real Sociedad Espaola de Física, 2016.

[6] Solar Turbines. Caterpillar. https://mysolar.cat.com/cda/files/126873/7/dsm50pg.pdf.

[7] R. Chacartegui, J.M. Muñoz de Escalona, D. Sánchez, B. Monje, and T. Sánchez. Alternative cycles based on carbon dioxide for central receiver solar power. *Appl. Thermal Eng.*, 31:872–879, 2011.

[8] M. Romero, R. Buck, and .E. Pacheco. An update on solar central receiver systems, projects, and technologies. *Transactions of the ASME*, 124:98, 2002.

[9] Meteosevilla. http://www.meteosevilla.com.